Medical Robots, Constrained Robot Motion Control, and "Virtual Fixtures"

(Part 3)

Russell H. Taylor
601.455/655

Disclosures & Acknowledgments

- **<u>This is the work of many people</u>**
- Some of the work reported in this presentation was supported by fellowship grants from Intuitive Surgical and Philips Research North America to Johns Hopkins graduate students and by equipment loans from Intuitive Surgical, Think Surgical, Philips, Kuka, and Carl Zeiss Meditec.
- Some of the work reported in this talk incorporates intellectual property that is owned by Johns Hopkins University and that has been or may be licensed to outside entities, including including Intuitive Surgical, Varian Medical Systems, Philips Nuclear Medicine, Galen Robotics and other corporate entities. Prof. Taylor has received or may receive some portion of the license fees. Also, Dr. Taylor is a paid consultant to and owns equity in Galen Robotics, Inc. These arrangements have been reviewed and approved by JHU in accordance with its conflict of interest policy.
- Much of this work has been funded by Government research grants, including NSF grants EEC9731478 and IIS0099770 and NIH grants R01-EB016703, R01-EB007969, R01-CA127144, R42-RR019159, and R21-EB0045457; by Industry Research Contracts, including from Think Surgical; by gifts to Johns Hopkins University from John C. Malone, Richard Swirnow and Paul Maritz; and by Johns Hopkins University internal funds.

Single Port Access Surgery

Nabil Simaan (Vanderbilt, Columbia), with
P. Allen (Columbia), D. Fowler (Columbia)

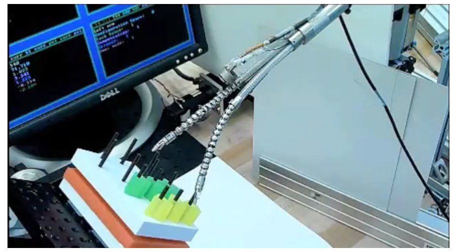

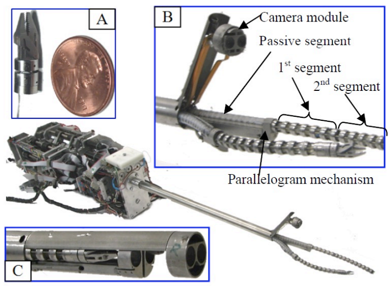

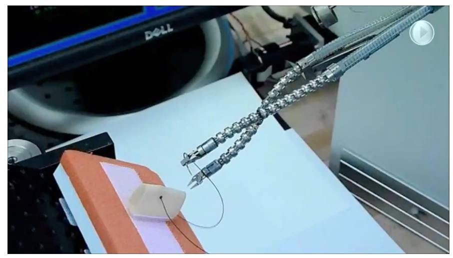

New technology finally allows true evaluation of the potential of single port access surgery. Systems raise new questions about control and telemanipulation infrastructure/cooperative control.

Single Port Access Robotic Surgery

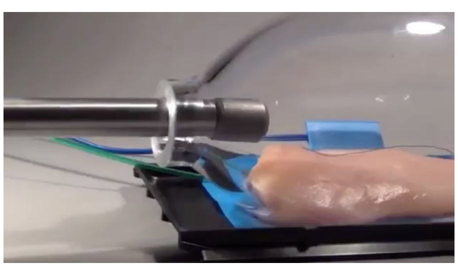

Titan Medical Sport
https://www.youtube.com/watch?v=jIvjvcKA6xQ

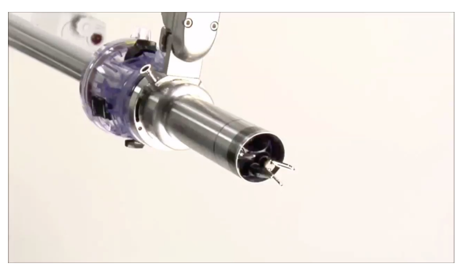

Intuitive Surgical Sp
https://www.youtube.com/watch?v=-jm63JdTrp4

Robot-Assisted Skull Base Surgery

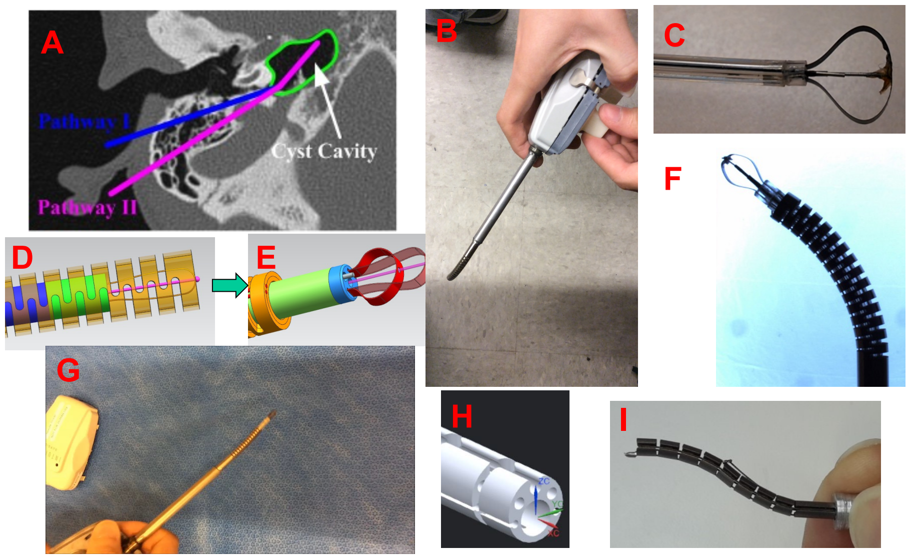

Integration of a Snake-like Dexterous Manipulator for Head and Neck Surgery with the da Vinci Research Kit

S. Coemert, F. Alambeigi, A. Deguet, J. P. Carey, M. Armand, T. C. Lueth, R. H. Taylor

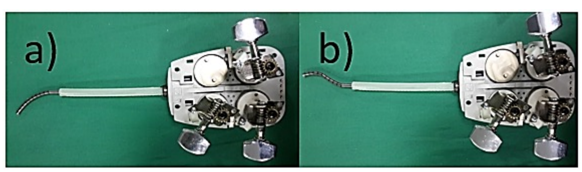

Handheld actuation concept: a) C-shaped b) S-shaped

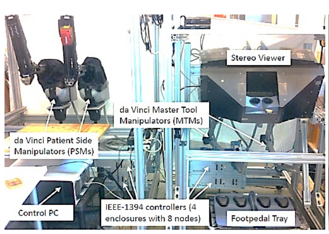

Overview of the DVRK system [5]

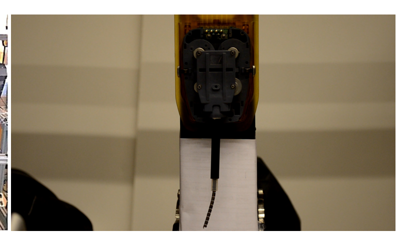

Video: Actuation of the SDM attached to DVRK

S. Coemert, F. Alambeigi, A. Deguet, J. P. Carey, M. Armand, T. C. Lueth, and R. H. Taylor, "Integration of a Snake-like Dexterous Manipulator for Head and Neck Surgery with the da Vinci Research Kit", in *Hamlyn Symposium on Medical Robotics*, London, June 26-27, 2016. pp. 58-59.

APL Large Lumen, Dexterous Snake for MIS

- Joint project with JHU APL
- Innovative fabrication process completely isolates drive cables
- Current prototypes
  - 2 DoF (C-bend) and 4DoF (S-bend)
  - Nitinol structure with high stiffness
  - 6 mm OD; Large 4 mm lumen allows insertion of surgical instruments
- Initial application: Minimally-invasive curettage of osteolytic lesions

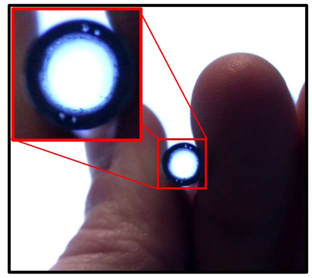

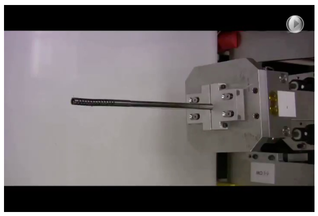

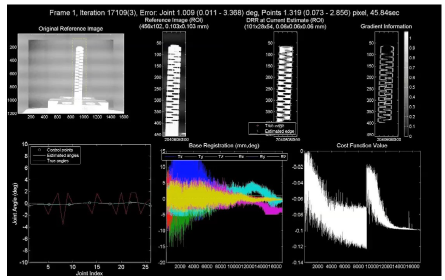

M. Armand, R. Taylor, M. Kutzer, R. Murphy, S. Segrett,i F. Alambeigi, I. Iordachita, H. Liu, Y. Otake *et al.*

Treatment of Osteolytic Lesions

- Indication: Osteolysis behind a well-fixed acetabular component
  - Leads to component loosening and failure of THA
- Surgical Goals
  - Minimally invasive removal of the osteolytic lesion
  - Treatment of the lysis without full replacement of the acetabular component
- Surgical Procedure
  - Access the lesion through the screw holes of the acetabular component (minimally invasive)
  - Remove and grafting the lesion
  - Replace the polyethylene liner

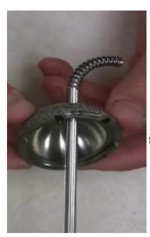

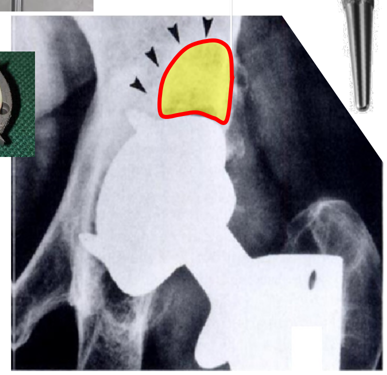

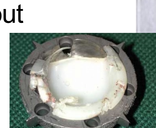

Minimally-Invasive Osteolysis Curettage

M. Armand, R. Taylor, M. Kutzer, R. Murphy, S. Segrett,i F. Alambeigi, I. Iordachita, H. Liu, Y. Otake P. Wilkening, *et al.*

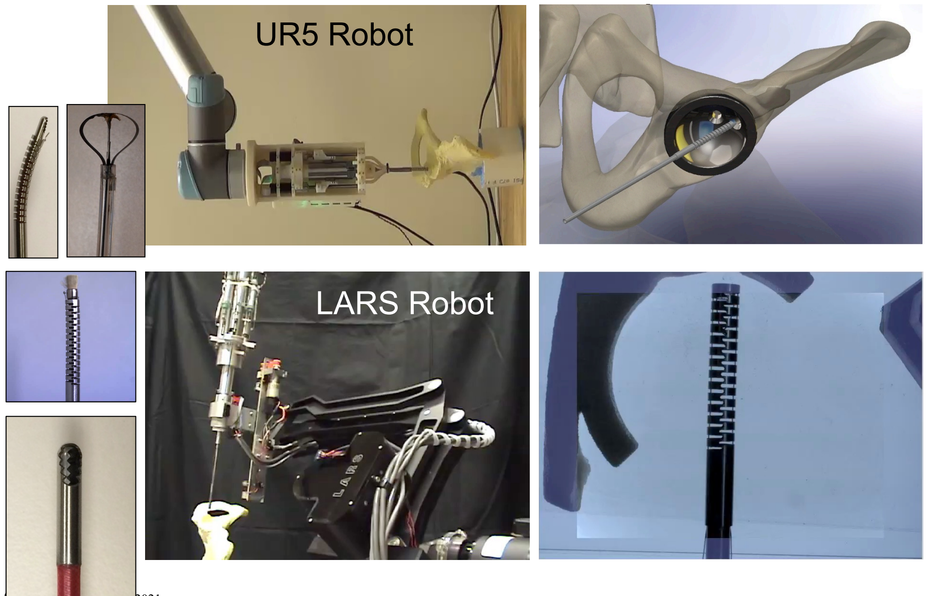

Novel Shape Sensor Array (SSA) for Large Curvature Detecting

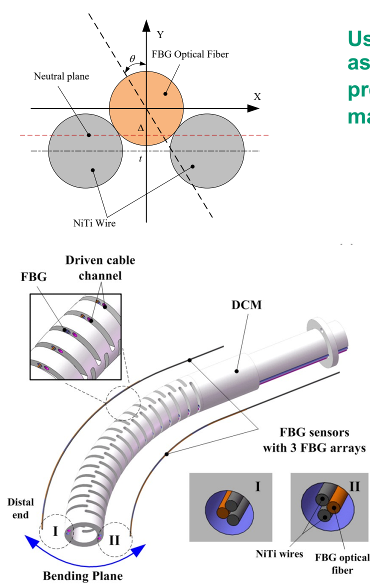

Using FBG sensors along with nitinol wires as the supporting substrates, we can prevent local stress concentration, therefore maximizing curvature detection range.

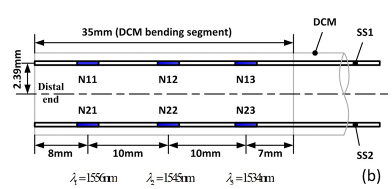

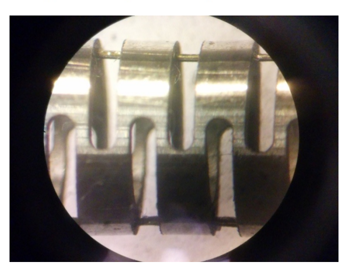

Hao Liu, Amirhossein Farvardin, Sahba Aghajani Pedram, Iulian Iordachita, Russell H. Taylor, Mehran Armand

Novel Shape Sensor Array (SSA) for Large Curvature Detecting

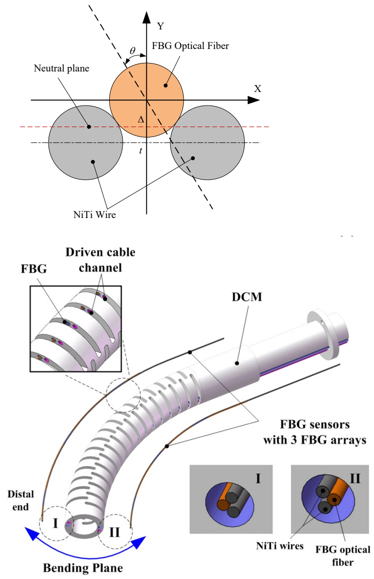

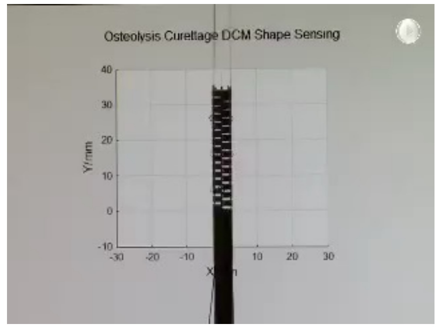

Hao Liu, Amirhossein Farvardin, Sahba Aghajani Pedram, Iulian Iordachita, Russell H. Taylor, Mehran Armand

11

Curved Drilling of the Femoral Head

Alambeigi, *et al.*

- Osteonecrosis of the femoral head
  - More than 20,000 patients per year
  - To reduce the pressure in the femoral head, core decompression was developed more than three decades ago.
- Steerable "snake" with flexible drill provides better

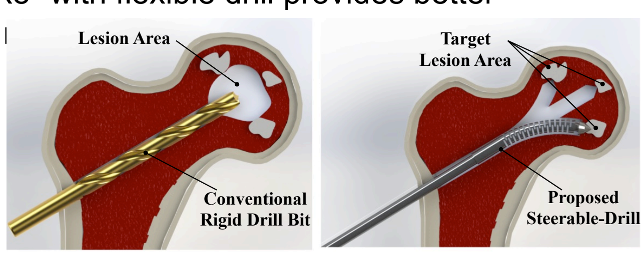

Farshid Alambeigi, Yu Wang, Shahriar Sefati, Ryan. J. Murphy, Iulian Iordachita, Russell H. Taylor, Harpal Khanuja, and Mehran Armand, "Curved-Drilling Approach in Core Decompression of the Femoral Head Osteonecrosis Using a Continuum Manipulator", *Proc. ICRA 2017*

12

Curved Drilling of the Femoral Head

Alambeigi, *et al.*

- Sample Holder Mechanism: feeding motion and 6DOF force se
- Thermal Camera: "Real-time" tracking of the cutter

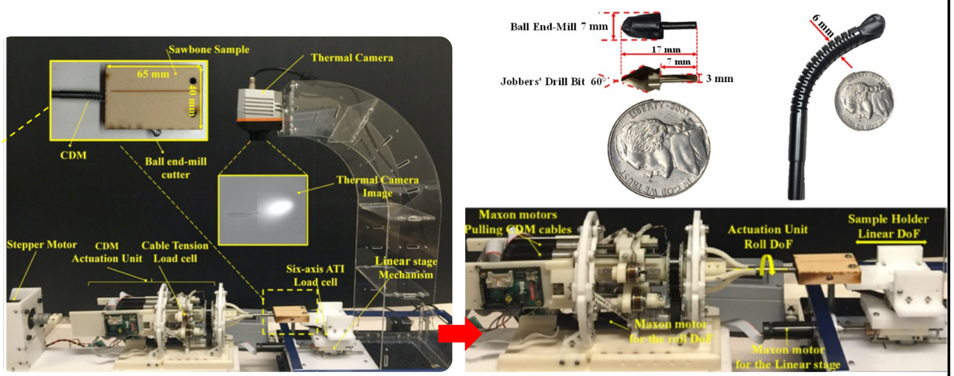

Farshid Alambeigi, Yu Wang, Shahriar Sefati, Ryan. J. Murphy, Iulian Iordachita, Russell H. Taylor, Harpal Khanuja, and Mehran Armand, "Curved-Drilling Approach in Core Decompression of the Femoral Head Osteonecrosis Using a Continuum Manipulator", *Proc. ICRA 2017*

Curved Drilling of the Femoral Head

Alambeigi, *et al.*

S-Shape and multiple branch curved-drilling

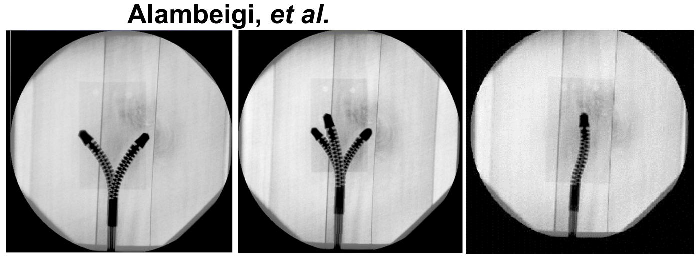

Curved-Drilling Experiments on human cadaver specimens

Farshid Alambeigi, Yu Wang, Shahriar Sefati, Ryan. J. Murphy, Iulian Iordachita, Russell H. Taylor, Harpal Khanuja, and Mehran Armand, "Curved-Drilling Approach in Core Decompression of the Femoral Head Osteonecrosis Using a Continuum Manipulator", *Proc. ICRA 2017*

Challenges in Precise Minimally Invasive Head- and Neck Surgery

- Long (25cm) instruments
  - amplify hand tremor
  - reduce precision
- Tight spaces near sensitive anatomy
- Limited working area

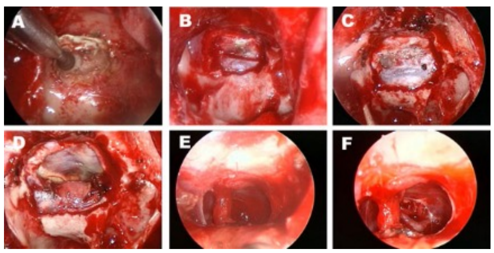

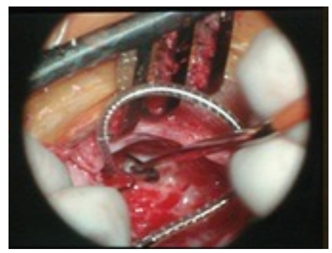

15 601.455/655 Fall 2021

The Robotic ENT Microsurgery System (REMS)

User interface:
- Hands-on control, surgeon "in the game"
- Foot pedal-controlled gain

Technical specs:
- Up to 0.025 mm precision on-demand
- 6 degrees of freedom
- 125x125x125mm work volume
- Calibrated accuracy ~50-150µm

Control modes:
- Free hand
- Remote center of motion
- Virtual fixture avoidance
- Teleoperation

K. Olds, *Robotic Assistant Systems for Otolaryngology-Head and Neck Surgery,* PhD thesis in Biomedical Engineering, Johns Hopkins University, Baltimore, March 2015.

16 601.455/655 Fall 2021

Playing the “Operation Game” with Long Instruments

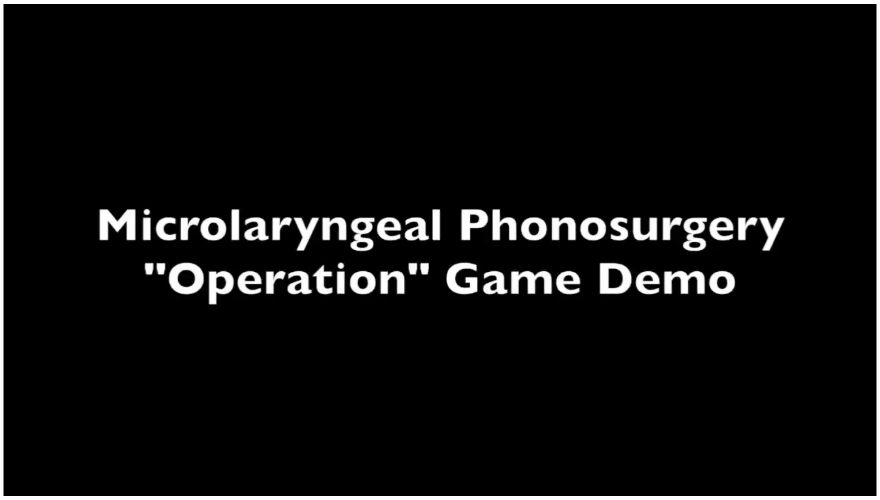

K. Olds, ***Robotic Assistant Systems for Otolaryngology-Head and Neck Surgery,*** **PhD thesis in Biomedical Engineering, Johns Hopkins University, Baltimore, March 2015.**

REMS Typical Applications

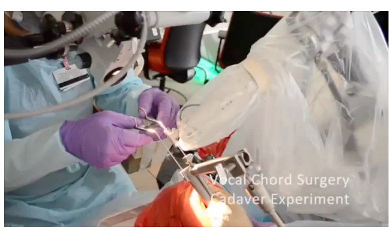

Laryngeal / Vocal Cord

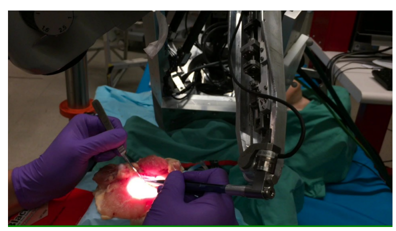

Open Microsurgery

Image-guided sinus surgery with virtual fixtures

Other applications include:

- Otology
  - Stapes surgery
  - Mastoidectomy
  - Cochlear implant
- Craniotomy
- Spine
- Hand
- …

Vitreoretinal Microsurgery

British Journal of Ophthalmology 2004 - Akifumi Ueno et al

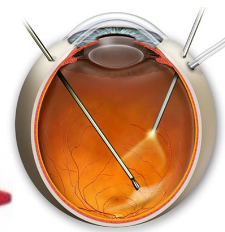

www.eyemdlink.com

Alcon Vitreosurgery Instrument

20 601.455/655 Fall 2021
Copyright R. H. Taylor

Engineering Research Center for Computer Integrated Surgical Systems and Technology

20

Microsurgery Assistant Workstation

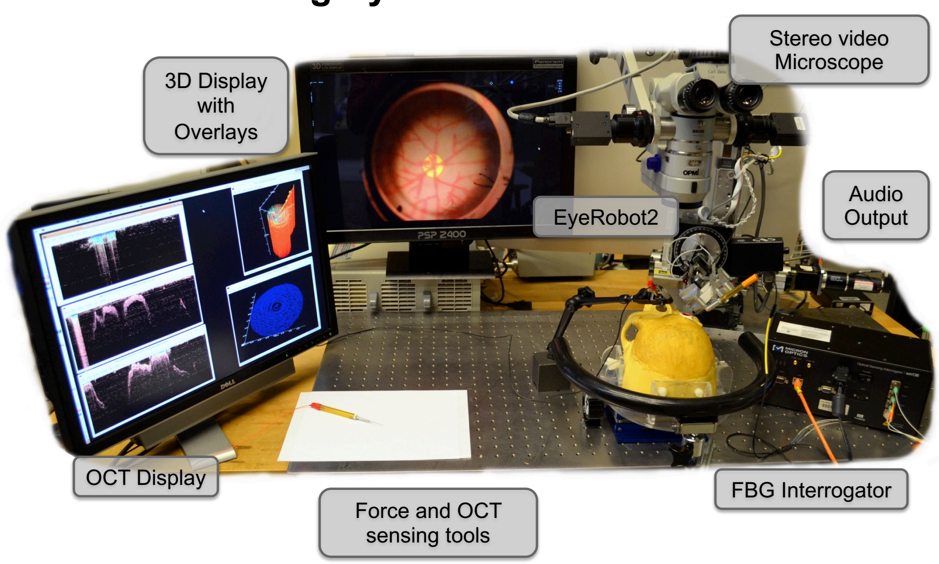

21 601.455/655 Fall 2021
Copyright R. H. Taylor

Engineering Research Center for Computer Integrated Surgical Systems and Technology

21

Retina Mosaicking, Annotation, and Registration

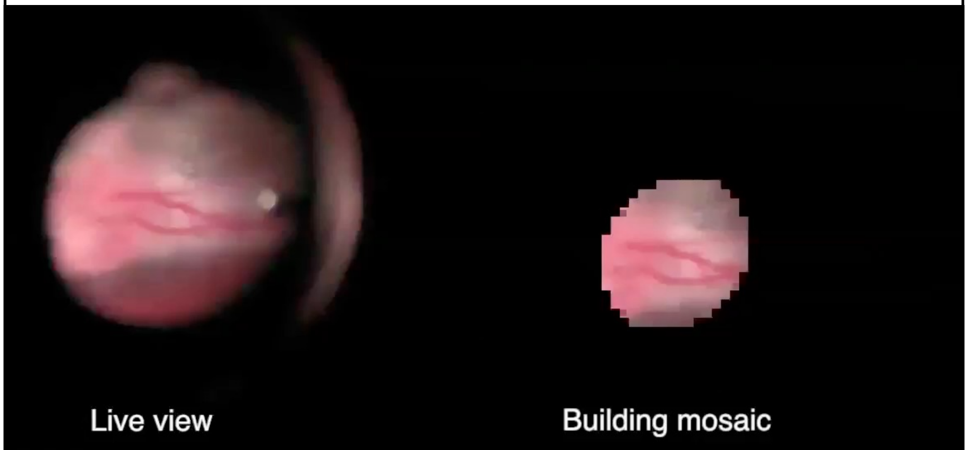

R. Richa, B. Vagvolgyi, R. Taylor, G. Hager, *MICCAI 2012*,

JHU Steady Hand "Eye Robot"

Russell Taylor, Iulian Iordachita, D. Gierlach, D. Roppenocker, *et al.*

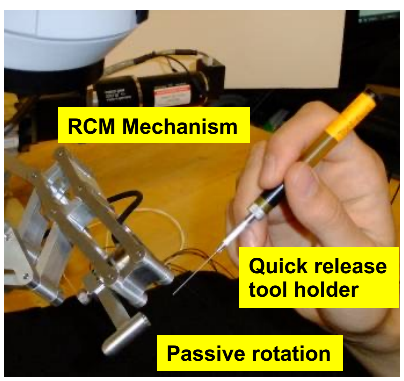

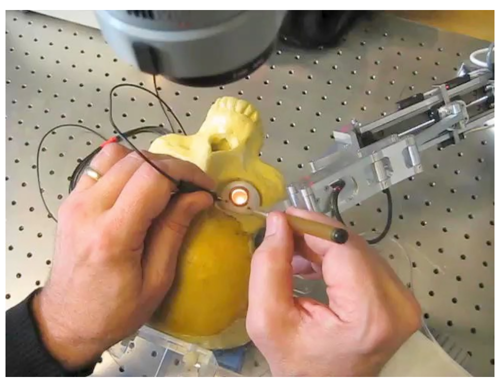

- Highly precise robot
- Hands-on cooperative control or teleoperation
- Several generations in lab

- Precise, stable platform for developing "smart" surgical instruments and sensors
- Virtual fixtures and advanced control

Retinal Microsurgery – *in vivo* experiments

- Overall System Performance
- System Ergonomics
- Collect Data
  - Robot / Force / OCT
  - Video / Audio

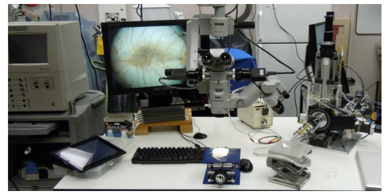

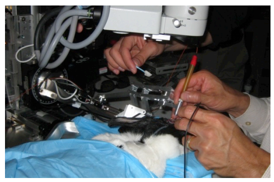

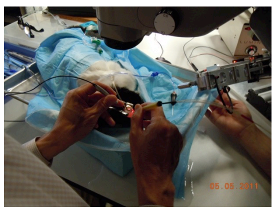

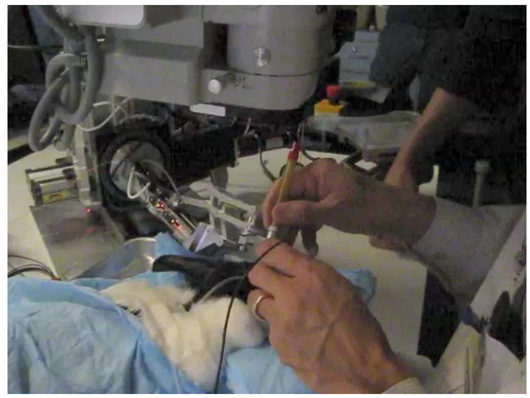

 601.455/655 Fall 2021

Engineering Research Center for Computer Integrated Surgical Systems and Technology

24

Force-Sensing Micro-Forceps Tools for Vitreoretinal Surgery

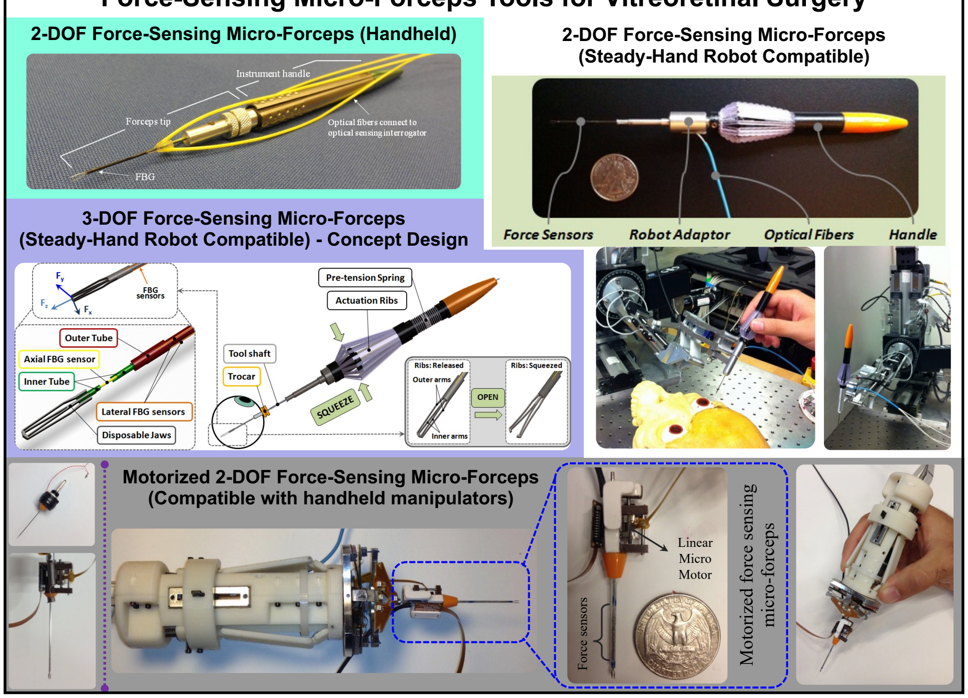

25

In-vivo experiments

- Test the force sensing micro-forceps in-vivo using rabbit in the operating room
- Force measurements, stereo microscopic video, and surgeon's voice annotation were recorded with timestamps for synchronization and analysis

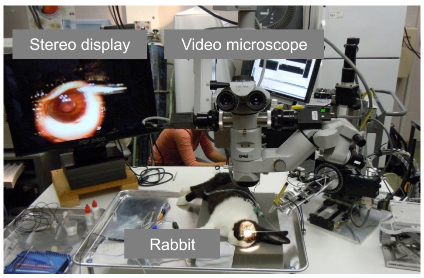

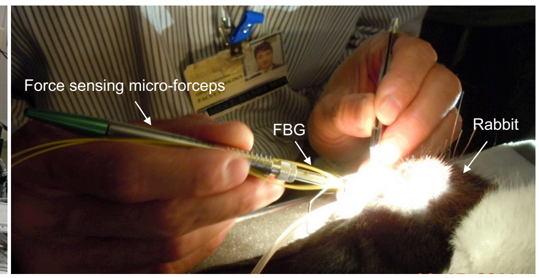

Xingchi He, Marcin Balicki, Jin U. Kang, Peter Gehlbach, James Handa, Russell Taylor, Iulian Iordachita
"Force sensing micro-forceps with integrated fiber Bragg grating for vitreoretinal surgery", SPIE 202

Video overlay of tool tip forces

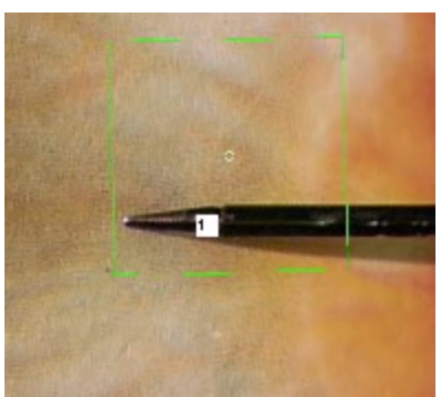

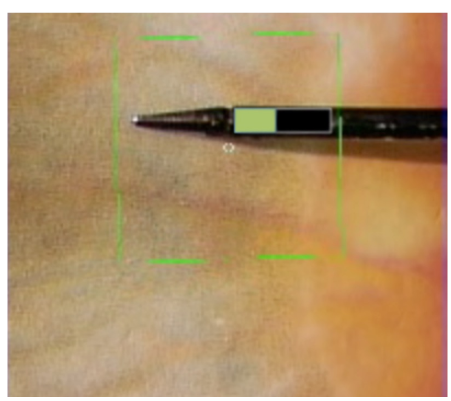

Use of Audio and Voice

- Voice commands and annotation
- Auditory sensory substitution

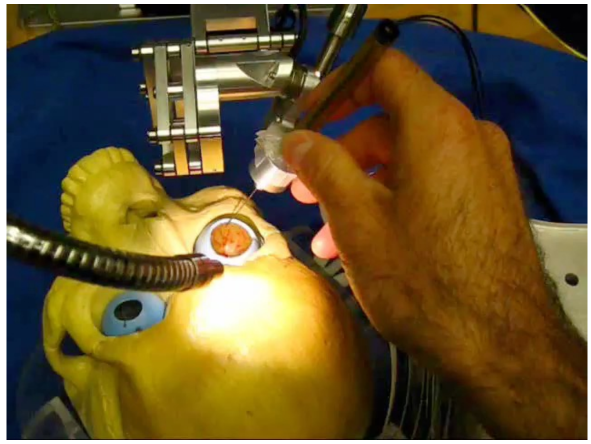

Example Audio Response to Force Input

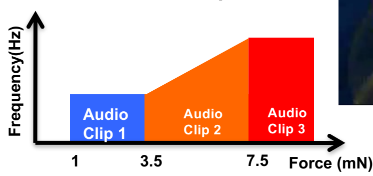

M. Balicki, *et al.*

Dual Force Sensor

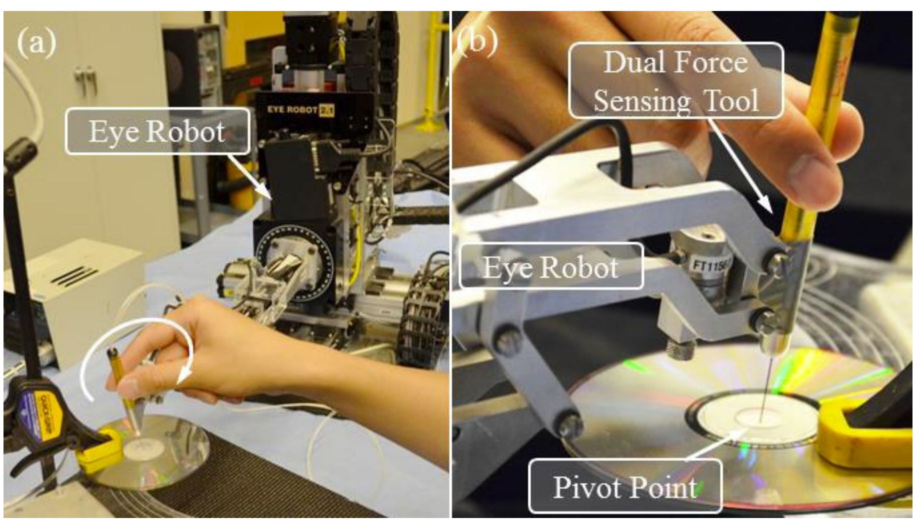

X. He, Marcin Balicki, P. Gehlbach, J. Handa, R. Taylo, and I. Iordachita, "Variable Admittance Robot Control with A New Dual Force Sensing Instrument for Retinal Microsurgery", *in IEEE Int. Conf. Rob. Automat*, Hong Kong, May 31-June 5, 2014..

Dual Force Sensor

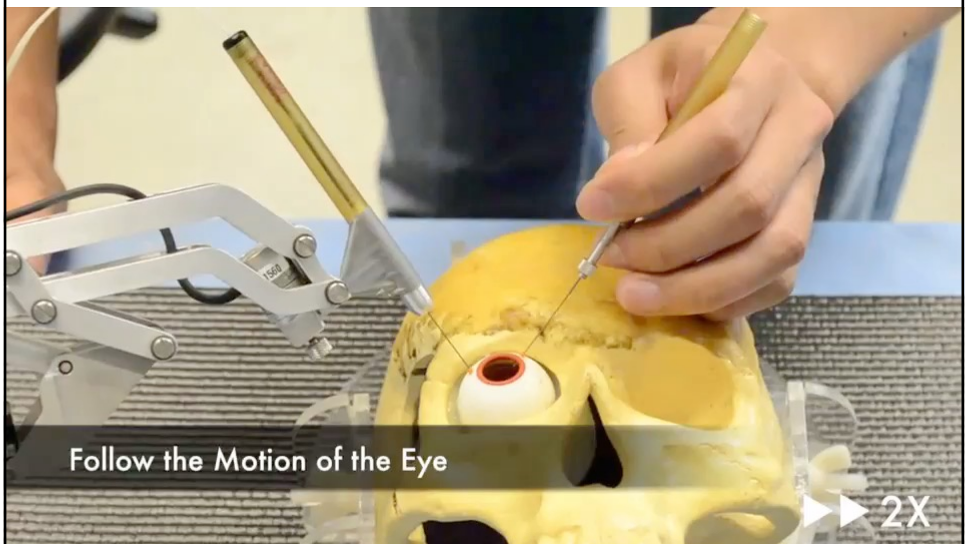

X. He, Marcin Balicki, P. Gehlbach, J. Handa, R. Taylo, and I. Iordachita, "Variable Admittance Robot Control with A New Dual Force Sensing Instrument for Retinal Microsurgery", *in IEEE Int. Conf. Rob. Automat*, Hong Kong, May 31-June 5, 2014..

μForce Scaling Cooperative Control

Cooperative Control

Velocity at the tool (V) is proportional to (α gain) the user's input force at the handle (F_h)

$$\dot{x} = \alpha F_h$$

μForce Scaling

Amplifies (ϒ gain) the human-imperceptible forces sensed at the tool tip (F_t) to handle interaction forces (F_h) by modulating robot velocity.

$$\dot{x} = \alpha\left(F_h - \gamma F_t\right), \quad \text{e.g., } \gamma = 500$$

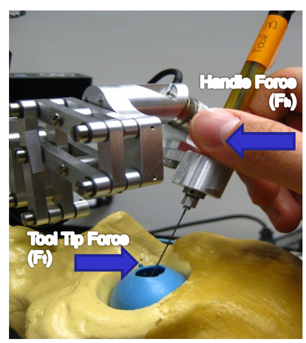

Kumar et al (ICRA' 00) ; Balicki et al. (MICCAI'10); Uneri et al., BioRob 2010

µForce Guided Cooperative Control

- ¬ User fights against ever increasing resistance
- ✓ Ensure safety tip force limits
- ¬ User interaction is limited at high-resistance regions
- ✓ Try to avoid those regions for later peeling
- ¬ User gets “stuck”, gives up, tries re-approach
- ✓ Ensure continuous user motion, even at the boundaries

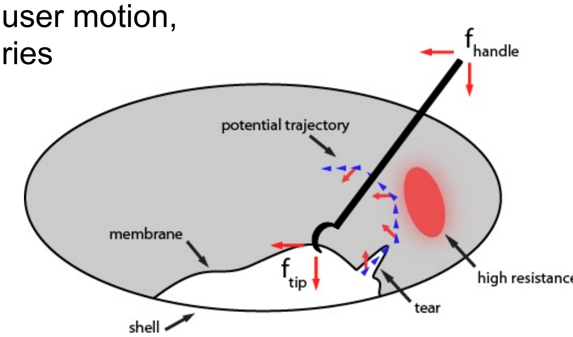

Uneri *et al.*, BioRob 2010

µForce Guided Cooperative Control

- Global Limiting
  - Task-specific tip force limit
  - User controlled limit distribution
- Continuous motion at the constraint boundaries
- Virtual spring construct to ensure stability

$$f_{lim} = f_{max} \frac{|f_h|}{\|f_h\|}$$

$$\dot{x}_{lim} = \dot{x}\left(\frac{f_{lim} - |f_t|}{f_{spring}}\right)$$

Local Force Minimization

- Guiding user towards direction of minimum resistance
- Sensitivity variable allows user override
- Haptically intuitive response
- Avoids / postpones reaching limits

$$\dot{x}_{min} = k_p\left(1 - s\frac{|f_t|}{\|f_t\|}\right) f_h$$

Uneri *et al.*, BioRob 2010

Experimental Platform

Focusing on:

•Properties of the tissue we interact with

•The method of interaction, i.e. performance of our algorithms

Performed on:

- **Inner shell membrane of raw eggs**
- **Surrogate tissue for epiretinal membrane peeling**

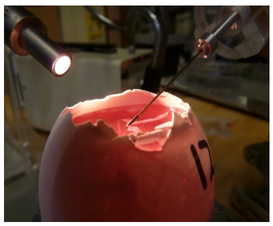

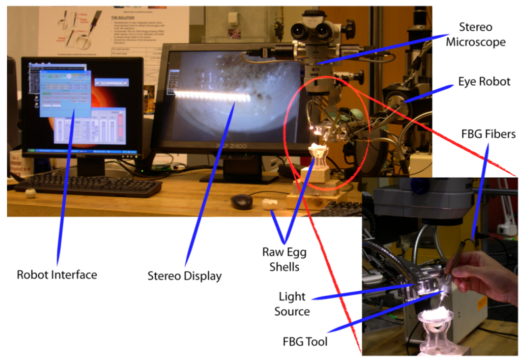

Uneri *et al.*, BioRob 2010

Experiment: Tissue Force Characterization

- A corrected position allows us to observe tissue strain
- Controlled constant force application
  - Incremented by 1mN, with 10s delay, over a range of 1-10mN
- Characteristic curve obtained reveals a similar pattern to those seen in fibrous tissue tearing
  - Toe region: Safe
  - Linear region: Predictive
  - Failure region: Peeling

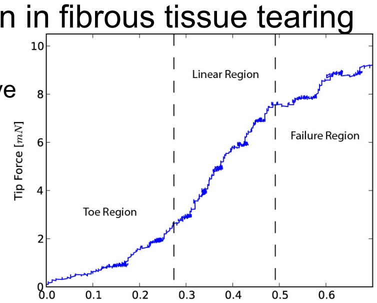

Uneri *et al.*, BioRob 2010

Experiment: Tissue Force Characterization

- A corrected position allows us to observe tissue strain
- Controlled constant force application
  – Incremented by 1mN, with 10s delay, over a range of 1-10mN
- Characteristic curve obtained reveals a similar pattern to those seen in fibrous tissue tearing
  – Toe region: Safe
  – Linear region: Predictive
  – Failure region: Peeling

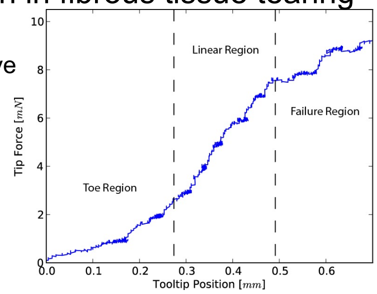

Uneri *et al.*, BioRob 2010

Enhanced Cooperative Control Peeling Algorithm

The algorithm biases operator-robot interaction towards the direction of least tissue resistance while limiting forces.

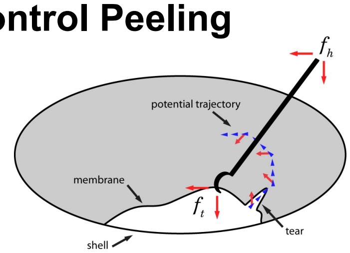

Tape Phantom Peeling

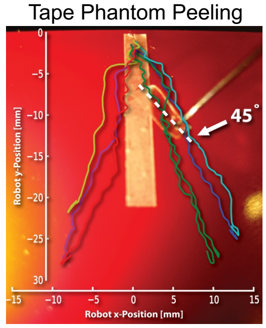

Peeling angles converge to 45 °

Inner Egg Shell Membrane Peeling

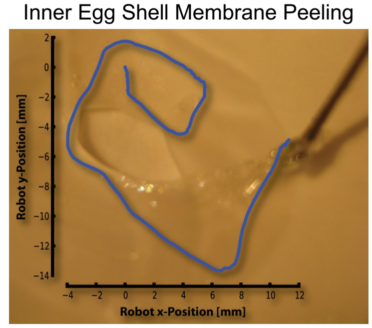

Resulting motion pattern resembles commonly used capsulorhexis technique

Uneri *et al.*, BioRob 2010

Experiment:
μForce Guided Cooperative Control

- Task: delaminate PVC strip with acrylic adhesive from a wax surface.
- Strip is peeled at an average of 45˚
- User was guided away from the centerline in the direction of lowest resistance

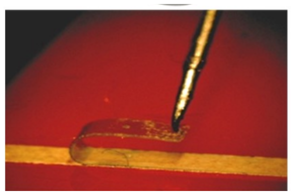

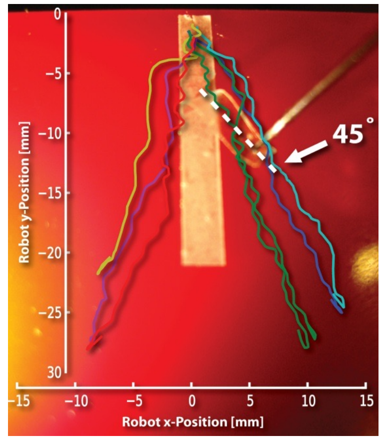

Uneri *et al.*, BioRob 2010

Experiment:
μForce Guided Cooperative Control

- Goal: Remove a section of egg inner shell membrane
- Circular trajectory consistent with the results from the strip peeling experiment
- Magnify the perception of tip forces lateral to direction of desired motion
- Results in a peel pattern seen Capsulorhexis maneuver

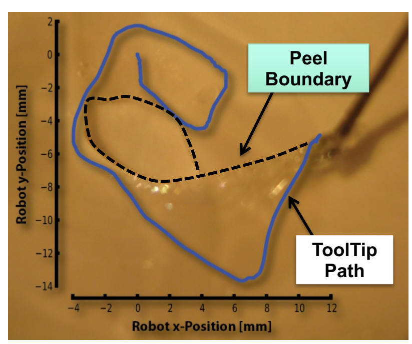

Peeling Inner Egg Shell Membrane

Uneri *et al.*, BioRob 2010

Imaging (OCT) Built Into 0.5mm Surgical Tool

M. Balicki, J. Han, X. Liu, I. Iordachita, P. Gehlbach, J. Handa, R. Taylor, J. Kang.

- Fourier Domain Common Path OCT (FD CPOCT)
- Combined Superluminescent Diodes
- Functional and structural images

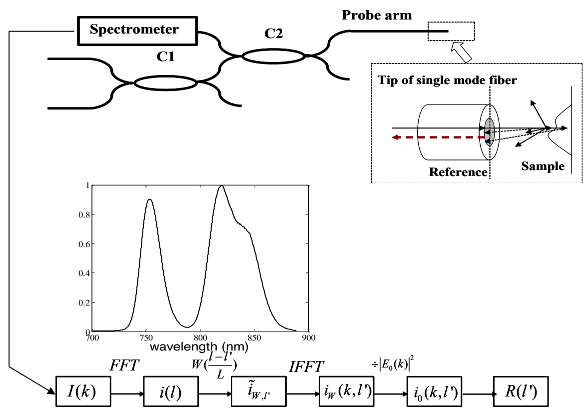

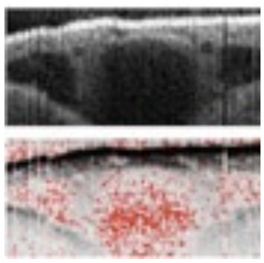

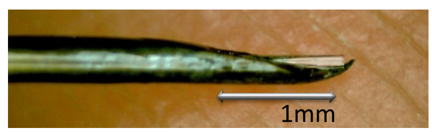

Autonomous Surface Following

M. Balicki, J.-H. Han, I. Iordachita, P. Gehlbach, J. Handa, R. H. Taylor, and J. Kang, *MICCAI 2010*

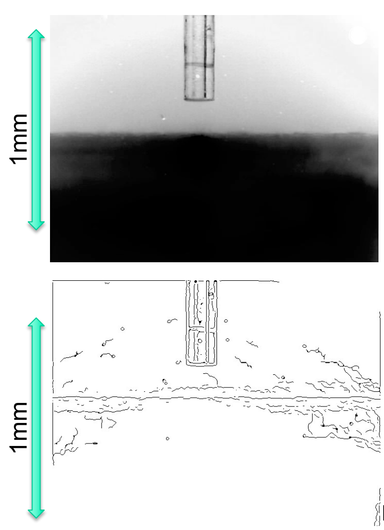

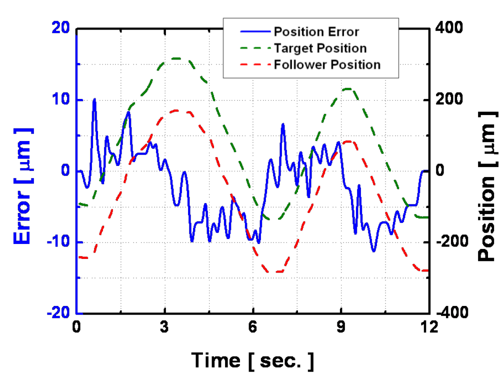

* 500 µm/s Velocity Limit

Noise Rem. /Thresholded/Canny

OCT-feedback in fast hand-held robot

J. Kang, P. Gehlbach, R. Taylor, *et al.*

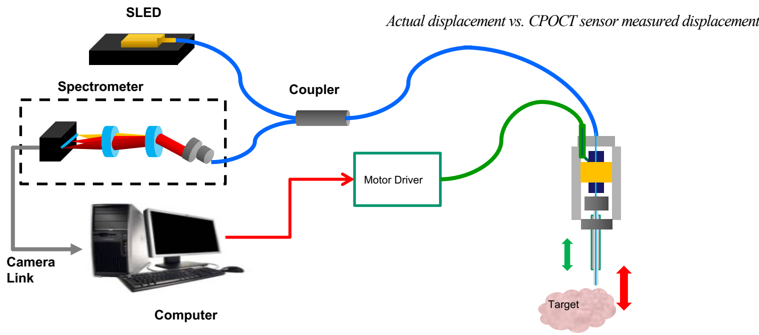

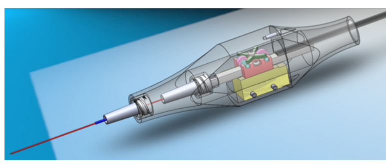

42 601.455/655 Fall 2021
Copyright R. H. Taylor
Engineering Research Center for Computer Integrated Surgical Systems and Technology

42

Safety Barrier

J. Kang, P. Gehlbach, R. Taylor, *et al.*

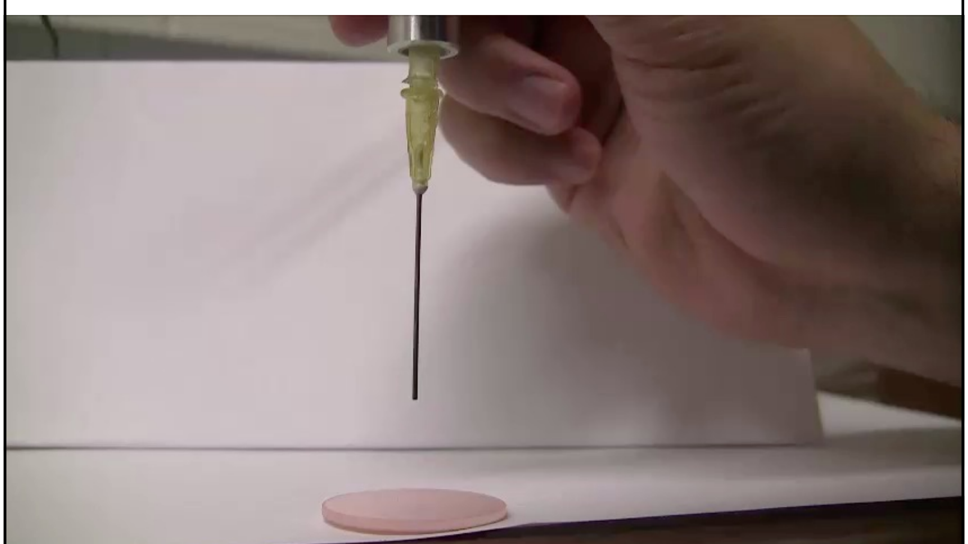

43 601.455/655 Fall 2021
Copyright R. H. Taylor
Engineering Research Center for Computer Integrated Surgical Systems and Technology

43

Smart Micro-Forceps

J. Kang, P. Gehlbach, R. Taylor, *et al.*

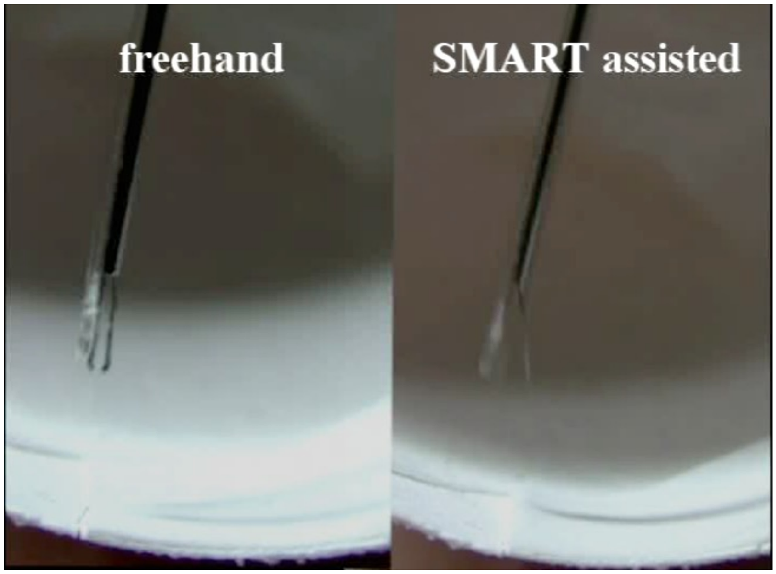

OCT-servoed Injections

J. U. Kang, G.W. Cheon, and P. Gehlbach

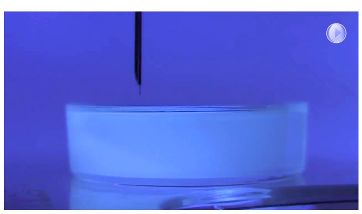

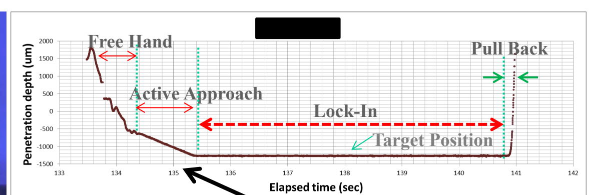

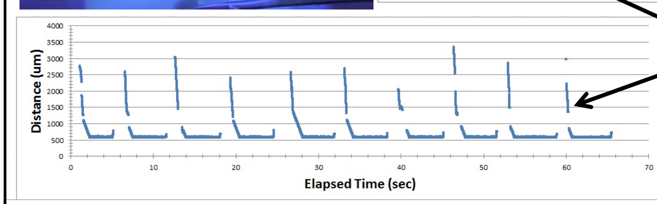

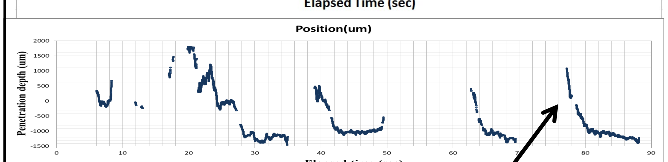

Robot+OCT

Freehand

Gyeong Woo Cheon, Yong Huang, Hye Rin Kwag, Ki-Young Kim, Russell H. Taylor, Peter Gehlbach, Jin U. Kang, "Injection-depth-locking axial motion guided handheld micro-injector using CP-SSOCT," 36th Annual International IEEE EMBS Conference, 1753, August 2014

GW Cheon, Y Huang, JU Kang, "Active depth-locking handheld micro-injector based on common-path swept source optical coherence tomography," SPIE BiOS, 93170U-93170U-5, 2015.

Robotically-Assisted Insertion of Cochlear Implants

- Setup
  - Phantom cochlea
  - Stiffer stylet
- Surgeon and novice inserted implants into phantom using three methods:
  - Manual insertion
  - Robot-assisted insertion
  - Robot-assisted insertion with virtual fixtures enacted

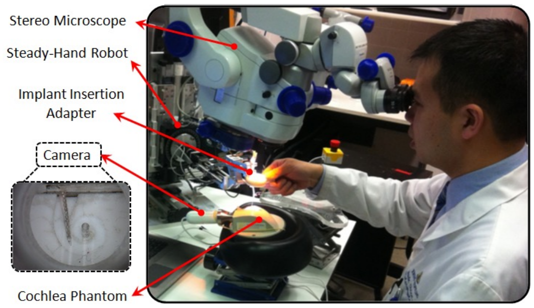

P. Wilkening, W. Chien, B. Gonenc, J. Niparko, J. U. Kang, I. Iordachita, and R. H. Taylor, "Evaluation of Virtual Fixtures for Robot-Assisted Cochlear Implant Insertion", in *IEEE Biomedical Robotics and Biomechanics (BioRob)*, Sao Paulo, 12-15 Aug, 2014. pp. 332-338.

Robotically-Assisted Insertion of Cochlear Implants

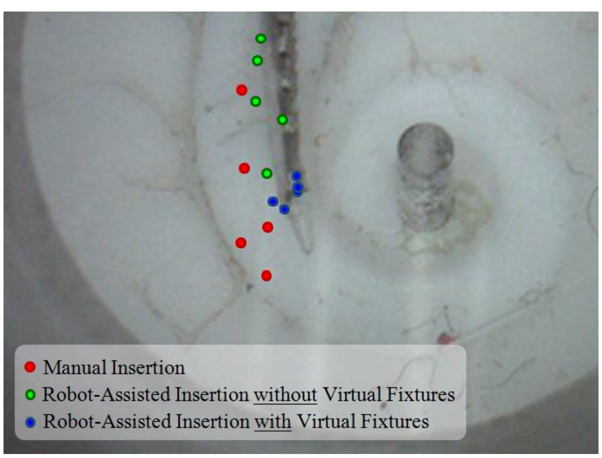

Novice's deployment points

- Each point represents the deployment point reached using one of the insertion methods
- Manual spread very far, not very accurate
- Robot-assisted also spread far, closer to center
- Robot-assisted with virtual fixtures closely clustered and highly accurate

P. Wilkening, W. Chien, B. Gonenc, J. Niparko, J. U. Kang, I. Iordachita, and R. H. Taylor, "Evaluation of Virtual Fixtures for Robot-Assisted Cochlear Implant Insertion", in *IEEE Biomedical Robotics and Biomechanics (BioRob)*, Sao Paulo, 12-15 Aug, 2014. pp. 332-338.

Robotically-Assisted Insertion of Cochlear Implants

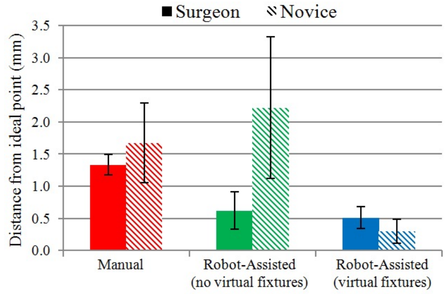

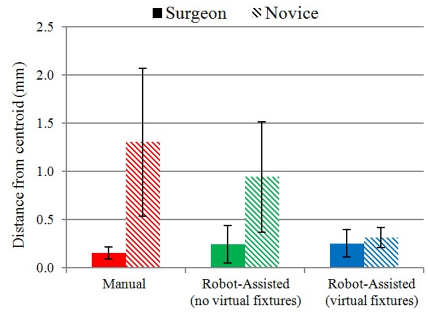

Accuracy Results

- Robot decreases surgeon's mean error by 0.7 mm
- Virtual fixture decreases novice's error by 1.4 mm
- 61.7% mean decrease in accuracy error using virtual fixtures

Repeatability Results

- Robot increased surgeon's repeatability by 0.1 mm
- Novice's repeatability decreased by 0.36 mm, then by 0.63 mm

P. Wilkening, W. Chien, B. Gonenc, J. Niparko, J. U. Kang, I. Iordachita, and R. H. Taylor, "Evaluation of Virtual Fixtures for Robot-Assisted Cochlear Implant Insertion", in *IEEE Biomedical Robotics and Biomechanics (BioRob)*, Sao Paulo, 12-15 Aug, 2014. pp. 332-338.

Information-enhanced robotic surgery

augmented reality displays imaging

safety barriers shared control "virtual fixtures"

SAW

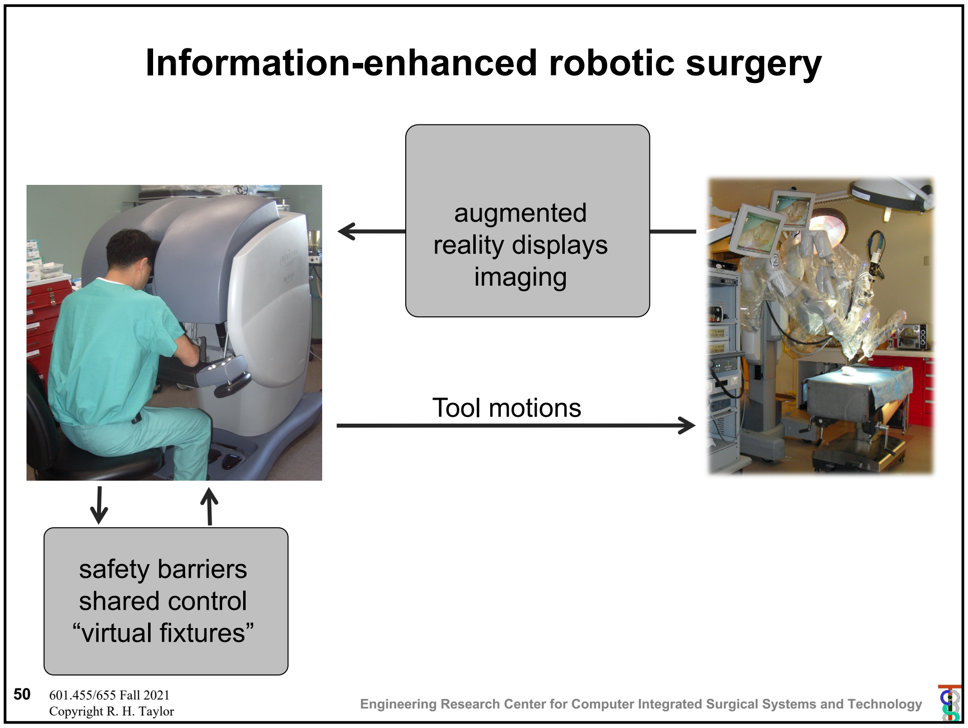
Information-enhanced robotic surgery
augmented reality displays imaging
Tool motions
safety barriers shared control “virtual fixtures”
50
601.455/655 Fall 2021
Copyright R. H. Taylor
Engineering Research Center for Computer Integrated Surgical Systems and Technology

50

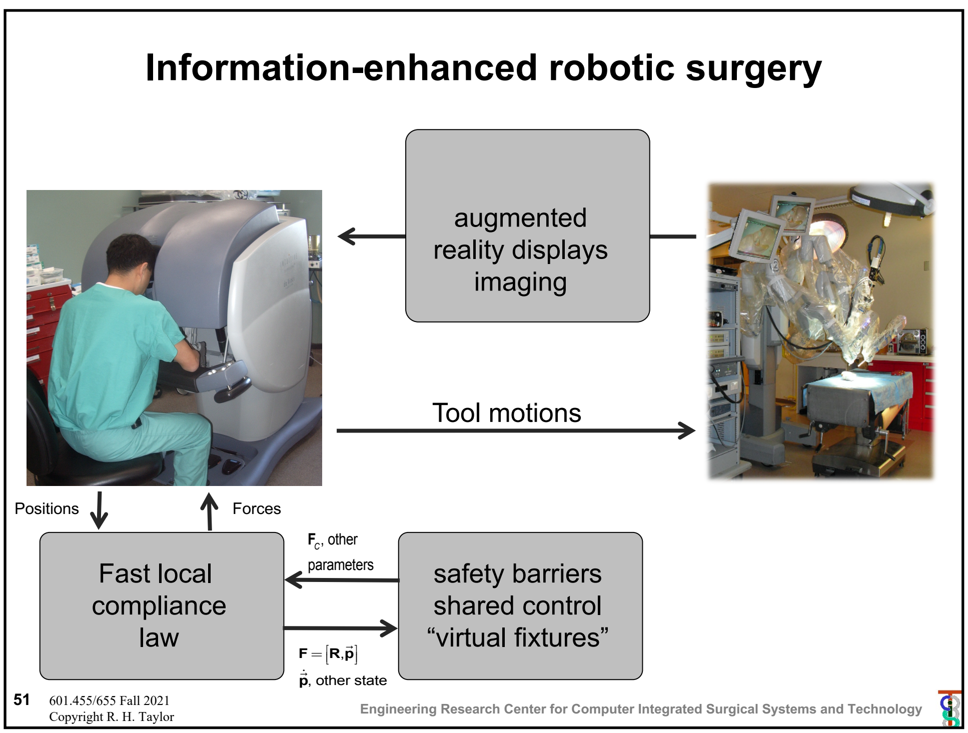
Information-enhanced robotic surgery
augmented reality displays imaging
Tool motions
Positions
Forces
Fast local compliance law
F_c, other parameters
$F = [R, \vec{p}]$
$\dot{\vec{p}}$, other state
safety barriers shared control “virtual fixtures”
51
601.455/655 Fall 2021
Copyright R. H. Taylor
Engineering Research Center for Computer Integrated Surgical Systems and Technology

51

Virtual Fixture "Hook" in DaVinci API

- **Experimental interface not in any clinical or commercial product.**
- Specification developed jointly by JHU and Intuitive to support research
- Prototyped at JHU by Tian Xia and Russ Taylor
- Current version implemented in DaVinci "S" model by Lawton Verner at ISI, with "hooks" in a proprietary ISI Application Program Interface
- Accessed through cisst/SAW libraries

Compliance virtual fixtures

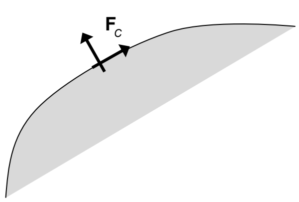

$$\mathbf{F} = [\mathbf{R}, \vec{\mathbf{p}}] = \text{current pose; } \dot{\mathbf{p}} = \text{current velocity}$$

$$\mathbf{F}_c = [\mathbf{R}_c, \vec{\mathbf{p}}_c] = \text{ position compliance frame}$$
$$\vec{\mathbf{k}}^{(+)}, \vec{\mathbf{k}}^{(-)} = \text{ position stiffness factors}$$
$$\vec{\mathbf{b}}^{(+)}, \vec{\mathbf{b}}^{(-)} = \text{ damping factors}$$
$$\vec{\mathbf{g}}^{(+)}, \vec{\mathbf{g}}^{(-)} = \text{ force bias terms}$$

$$\mathbf{R}_o = \text{orientation compliance frame}$$
$$\vec{\mathbf{k}}_o^{(+)}, \vec{\mathbf{k}}_o^{(-)} = \text{orientation stiffness factors}$$
$$\vec{\tau}^{(+)}, \vec{\tau}^{(-)} = \text{torque bias terms}$$

$$t = \text{time remaining on timeout counter}$$

Compliance virtual fixtures

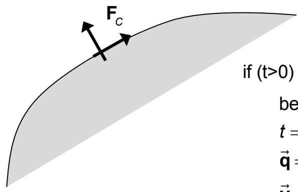

if (t>0) then

begin

$t = t - 1$

$\vec{\mathbf{q}} = \mathbf{F}_C^{-1}\vec{\mathbf{p}} = \mathbf{R}_C^{-1}(\vec{\mathbf{p}} - \vec{\mathbf{p}}_c)$

$\vec{\mathbf{v}} = \mathbf{R}_C^{-1}\dot{\vec{\mathbf{p}}}$

$\vec{\mathbf{h}} = \vec{\mathbf{0}};\ \vec{\psi} = \vec{\mathbf{0}}$

for $i \in \{x, y, z\}$ do

$\left\{\text{if } \vec{\mathbf{q}}_i \le 0 \text{ then } \vec{\mathbf{h}}_i = \vec{\mathbf{g}}_i^{(-)} + \vec{\mathbf{k}}_i^{(-)}\vec{\mathbf{q}}_i + \vec{\mathbf{b}}_i^{(-)}\vec{\mathbf{v}}_i \text{ else } \vec{\mathbf{h}}_i = \vec{\mathbf{g}}_i^{(+)} + \vec{\mathbf{k}}_i^{(+)}\vec{\mathbf{q}}_i + \vec{\mathbf{b}}_i^{(+)}\vec{\mathbf{v}}_i\right\};$

$\vec{\mathbf{f}} = \mathbf{R}_c\vec{\mathbf{h}}$; add $\vec{\mathbf{f}}$ to the forces exerted on the master

$\vec{\theta} =$ Rodrigues vector corresponding to $\Delta\mathbf{R} = \mathbf{R}_o^{-1}\mathbf{R}$

for $i \in \{x, y, z\}$ do

$\left\{\text{if } \vec{\theta}_i \le 0 \text{ then } \vec{\psi}_i = \vec{\tau}_i^{(-)} + \vec{\mathbf{k}}_i^{(-)}\vec{\theta}_i \text{ else } \vec{\psi}_i = \vec{\tau}_i^{(+)} + \vec{\mathbf{k}}_i^{(+)}\vec{\theta}_i\right\};$

add $\mathbf{R}_o\vec{\psi}$ to the torques exerted on the master

end

Surface following virtual fixture

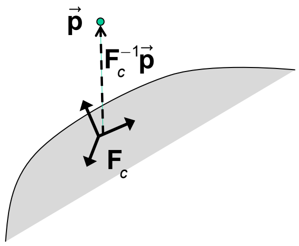

Goal: Stay on a surface; bias force drawing toward the surface; spring force resisting penetration

$\vec{\mathbf{p}}_c =$ closest point on surface

$\mathbf{R}_c\vec{\mathbf{z}} =$ surface normal at $\vec{\mathbf{p}}_c$

$\vec{\mathbf{k}}^{(-)} = [0, 0, -\textit{stiffness}]$

$\vec{\mathbf{g}}^{(+)} = [0, 0, -\textit{bias}]$

$\textit{Others} = 0$

Limitation and Extensions

- The specific abstraction just presented has some limitations. In particular, it separates the position and orientation compliance in a way that makes coupling of orientations and translations non-trivial.
- This can be gotten around to some extent by continually updating the virtual fixture compliance parameters.
- There are several obvious extensions that may be tried. For example, one can provide fuller matrices for virtual fixture force/torque generation. For example:

Compute $\vec{\mathbf{q}},\vec{\mathbf{v}},\vec{\theta},\vec{\phi}$ from $\mathbf{F}_c$ and $\mathbf{R}_o$, *where* $(\vec{\phi} = d\vec{\theta} / dt)$

Compute a region i of local configuration space from $\vec{\mathbf{q}}$ and $\vec{\theta}$

$$\begin{bmatrix} \vec{\mathbf{h}} \\ \vec{\psi} \end{bmatrix} = \mathbf{K}_i \bullet \begin{bmatrix} \vec{\mathbf{q}} \\ \vec{\theta} \end{bmatrix} + \mathbf{B}_i \bullet \begin{bmatrix} \vec{\mathbf{v}} \\ \vec{\phi} \end{bmatrix} + \begin{bmatrix} \vec{\mathbf{g}}_i \\ \vec{\tau}_i \end{bmatrix}$$

Add $\mathbf{R}_C\vec{\mathbf{h}}$ to master forces and $\mathbf{R}_0\vec{\psi}$ to master torques